International Journal of Innovative Research and Scientific Studies, 8(1) 2025, pages: 168-190

IJIRSS
International Journal of Innovative Research & Scientific Studies

ISSN: 2617-6548

URL: www.ijirss.com

Development of an intelligent geographic information system for mountain roads monitoring: Ground data collection and analysis

Gulnara Nurpeissova[1,2], Ainur Kairanbayeva[1*], Serik Nurakynov[1], Dina Panyukova[1,2], Kerey Panyukov[3]

[1]*Institute of Ionosphere, Almaty, Kazakhstan.*
[2]*Caspian University, Almaty, Kazakhstan.*
[3]*Satbayev University, Almaty, Kazakhstan.*

Corresponding Author: Ainur Kairanbayeva (*Email: kairanbaeva_a@ionos.kz*)

Abstract

This study examines the development of an intelligent geographic information system for mountain road monitoring. To make well-informed and timely management decisions in the planning, construction, and maintenance of mountain roads, and to anticipate potential critical situations and their effects on road conditions, it is imperative to employ modern methodologies. This study involves data collection from a specific section of a mountain road situated near Almaty, Kazakhstan. We gathered data on the road section through visual assessment, measurements of the coefficient of adhesion, and the acquisition of material samples from the structural layers of the roadbed. Based on the visual assessment and surface adhesion measurements, it became evident that the deformation of the studied road section, which includes a network of cracks and "non-standard" transverse cracks, is attributed to mountain mass shifts and water flows from slopes. Laboratory analysis of the collected samples revealed that excessive water saturation could result in cracks during freeze-thaw cycles, while a low resistance coefficient would lead to softening during humid conditions. An Intelligent Geographic Information System (IGIS) will incorporate the collected data alongside open remote sensing and weather data. The objective is to utilize this integrated system in the future for forecasting road conditions and maintenance requirements for similar roads in mountainous regions of the area. The measurements are carried out according to the state standards. That makes the system useful for government management purposes.

Keywords: Forecasting, Geographic information system, Landslide processes, Remote sensing, Road condition, Road construction material, Road pavement, Road survey data, Weather data.

DOI: 10.53894/ijirss.v8i1.3582
Funding: This research is supported by the Science Committee of the Ministry of Science and Higher Education of the Republic of Kazakhstan (Grant number: AP14971792&AP09260066).
History: Received: 1 February 2024/**Revised:** 23 August 2024/**Accepted:** 27 September 2024/**Published:** 7 October 2024

Competing Interests: The authors declare that they have no competing interests.
Authors' Contributions: Conceived and designed, data collection, V.C.N; analysis and interpretation of results, L.P.V; draft manuscript preparation by V.C.N and L.P.V. All authors have read and agreed to the published version of the manuscript.
Transparency: The authors confirm that the manuscript is an honest, accurate, and transparent account of the study; that no vital features of the study have been omitted; and that any discrepancies from the study as planned have been explained. This study followed all ethical practices during writing.
Institutional Review Board Statement: Not applicable.
Publisher: Innovative Research Publishing

1. Introduction

Transportation systems have a broad range of positive effects on both economic well-being and fairness, in addition to their role in lowering costs and enhancing investment, trade, and productivity. It serves as the lifeblood of any country's economy, and the sustainable functioning of transport infrastructure is a prerequisite for the nation's overall development [1]. Monitoring and maintaining the functionality of transportation systems is particularly challenging for large countries such as Kazakhstan [2].

Kazakhstan sprawls across a vast territory, spanning 2,724.9 thousand square kilometers, with an extensive road network covering 96,000 km. Within this network, the state-controlled roads encompass 25,000 km, boasting an impressive 89% in standard condition. Conversely, the local road network extends over 71,000 km, with 75% of its roads meeting the standard. The funding for maintenance, repair, and the modernization of the republican network is derived from the state budget, while the responsibility for the development, repair, and upkeep of local roads and the entire road network lies within the purview of local executive bodies [3].

The analysis of road surface condition data, as detailed in the article [4] was conducted to facilitate the effective implementation of a network-level road surface management program in Kazakhstan. The researchers underscored the significance of paved roads and transportation systems as vital assets for promoting political stability, economic growth, and sustainability in developing countries. Nevertheless, the presence of pavement backlogs and the high capital costs associated with road rehabilitation necessitate the use of pavement assessment tools to ensure the optimal return on investment.

Chinese scientists conducted a bibliometeric analysis using CiteSpace, which revealed that 96 countries actively engaged in research on the stability and reinforcement of soil foundations between 2005 and 2019, highlighting the significance of these studies. Among the various aspects of this research, the condition of the roadbed was consistently identified as a paramount concern in maintaining roadway integrity, with 211 research articles dedicated to this subject. These studies delved into the mechanisms and causes of roadbed issues, including deformation, settlement, longitudinal and transverse cracks, and more. Notably, various factors, including geographical, geological, and climatic characteristics, embankment height, layer thickness, base processing methods, groundwater levels, dynamic loading, and more, influence additional stresses on the roadbed. Among the various types of roads, those in mountainous areas are the most complicated due to the predominant influence of natural phenomena such as flash floods and landslides as well as extreme weather conditions. This insight underscores the vital role of understanding and mitigating such processes in ensuring the stability of mountain road infrastructure [5].

In the present study, the authors primarily focus on the examination of roads in mountainous regions. The recognition that around 14% of Kazakhstan's total land area is mountainous terrain motivates this research, as it necessitates a heightened focused on road infrastructure in these areas for the reasons stated above [6]. Recent international research on mountain roads offers valuable insights, as exemplified by the following studies.

In the article Luu, et al. [7] the extensive and destructive nature of flash floods and landslides in hilly regions along Vietnam's National Highway 6 is thoroughly examined. The findings indicate that the AdaBoost-RBF model excels in predicting relevant risks and providing management strategies. Similarly, the study Pradhan and Siddique [8] is about the stability of road cut slopes along India's National Highway-58 in the Himalayas.

Extreme weather conditions are also a significant contributor to road damage in mountainous areas. In a study by Wang et al. conducted in a northern mountainous region of China, the research highlighted substantial erosion on unpaved roads, emphasizing the need for comprehensive measures to address the growing erosion risks associated with extreme weather events [9].

Furthermore, in a review paper on fundamental approaches to predicting moisture damage in asphalt mixes, the authors suggest that moisture susceptibility is a primary cause of non-rigid pavement failures. However, it remains unclear which specific mechanism or combination of mechanisms leads to moisture damage and how it depends on factors such as temperature, mixture composition, binder aging, traffic volume, exposure duration to water, and potentially other road surface conditions [10].

In Kazakhstan, research in this field has been conducted within the framework of state programs over the past decade by KazdorNIILtd. The researchers from this scientific institution have identified key factors influencing the initiation and activation of geological hazards through extensive field research. Researchers have established that the presence of a slope, which represents relief energy, is a prerequisite for landslide development. Even under conditions of substantial rock moisture, the absence of such terrain features will prevent landslides from occurring. These various geological hazards can be categorized into seven groups, based on factors such as climate, biology, gravitational forces, surface and groundwater, freeze-thaw dynamics of rocks, and the utilization of subterranean spaces [11].

The acquisition of data related to road pavement surface damage represents a critical component in facilitating the pavement management process. It is essential to acknowledge that the structural condition of the road pavement significantly impacts its performance, and a comprehensive understanding of the structure's condition is imperative for effective road surface management, both at the network and project levels [12]. Employing a combination of non-destructive and destructive assessment methods offers a comprehensive understanding of the road surface's bearing capacity and strength. This information is instrumental in planning repair initiatives and assessing the necessity for infrastructure replacement or upgrades in the road network [13-15].

To investigate and forecast the condition of roads and railways in CIS countries, the primary approach involves diagnosing road and pavement conditions through road laboratories equipped with ground-penetrating radar (GPR) survey devices. In the USA and Europe, there is an increasing adoption of sensor systems for continuous road condition

monitoring [16, 17]. However, a drawback of these systems is their substantial financial requirements for system establishment and ongoing operation.

Satellite imagery and remote sensing technologies have achieved extensive global usage in optimizing land use, urban planning, and managing highway infrastructure [18-24]. These advanced techniques empower stakeholders to access current information regarding land conditions, natural resources, and infrastructure without the need for physical site visits, enabling swift responses to environmental changes and informed decision-making. In addition to their wide-ranging applications, these methods are particularly valuable for monitoring road and pavement conditions, planning and executing maintenance and repair initiatives, thus enhancing the overall efficiency and safety of road systems, especially in challenging terrains like mountainous areas, where environmental factors and geological conditions can significantly impact road stability and maintenance requirements.

In Kazakhstan, road surface condition prediction relies solely on data collected by mobile laboratories, which is accessible primarily to maintenance and design organizations. However, organizations responsible for local roads frequently face resource constraints that hinder their ability to conduct regular and comprehensive road diagnostics and make timely, informed decisions. Hence, the necessity arose for a methodology that could enable remote diagnostics and road condition forecasting utilizing publicly available data sources. We have initiated a project to develop an Intelligent Geographic Information System (IGIS) to predict road conditions in response. This system incorporates a combination of ground and satellite data, meteorological information, and computer modeling techniques. We select the Almaty-Kosmostation road as a case study for testing and implementing this system.

In the development and training of IGIS, meteorological data was sourced from an open database [25] covering the period from January 2016 to March 2023. The key factors taken into account from this dataset include air temperature, humidity, precipitation, and snow cover, as they are recognized as primary contributors to road deformation. Additionally, horizontal visibility and two types of cloudiness were considered indirect indicators of solar radiation, which can influence the road surface condition. The study employed archival images from the Sentinel-1 satellite spanning from 2017 to 2023 to process remote sensing data.

The manuscript primarily addresses the importance of collecting ground data related to road and pavement surface's technical and operational conditions, particularly through the use of mobile laboratories. The study delves into the methods, equipment, and findings associated with this effort, with specific focus on the Almaty-Kosmostation highway as a case study spanning the years 2021 to 2023.

2. Research Site and Location

The Almaty-Kosmostation highway crosses the Zailiysky Alatau and Northern Tien Shan high-mountainous regions. Its endpoint, the Kosmostation, is situated at the Zhusaly-Kezen pass (elevation: 3336 meters) and is the highest accessible point by car near Almaty. The Kosmostation itself comprises a complex of buildings and structures necessary for cosmic research, all strategically dependent on the quality of the highway for seamless operation.

As previously highlighted in the introduction, natural conditions, including terrain, soil composition, hydrogeological attributes, and climatic factors, have a profound influence on the performance and condition of road structures. Terrain largely dictates the predominant roadbed type, while the diversity of soil conditions hinges on soil stratum characteristics and soil type properties. Hydrogeological factors delineate the roadbed's positioning relative to groundwater levels, shaping the potential for groundwater infiltration, thereby influencing phenomena like landslides and heaving formations. Additionally, the topographical features constitute constant factors that delineate the dynamics and intensity of geological hazards (GH) within a given area. Depending on the terrain, gravitational forces give rise to two primary GH categories: those involving movement while maintaining contact with the slope and those involving movement with detachment from the slope. The former group encompasses phenomena such as landslides and avalanches, while the latter includes landslides and screes.

In the southeastern region of Kazakhstan, one encounters a series of mountain ranges belonging to the northern branch of the Tien Shan interspersed with intermountain depressions. These mountain ranges exhibit steep slopes intersected by profound gorges. The highest segments of these ridges feature a flat glacial topography, characterized by elevations with concentrated glaciers serving as sources for the contemporary hydrographic network and ranging between 4000-4500 meters above sea level. The geological composition predominantly comprises ancient sedimentary, igneous, and metamorphic rocks from the Lower Paleozoic era, encompassing materials such as sandstones, porphyries, granites, and gneisses. In contrast, the foothills and intermountain regions are predominantly shaped by Neogene and Quaternary deposits of glacial, alluvial, and proluvial-deluvial origin [26].

The region's territory falls within zones characterized by high seismic activity, with recorded tremor intensities ranging from 7 to 9 points. In this area, prevalent geological phenomena include erosion-mudflows, subsidence, deflationary processes, as well as land salinization and waterlogging [27, 28].

Debris flows transport substantial quantities of mudstone materials into the foothill zones and inclined plains, resulting in a significant surge in river runoff volume. In unprotected valleys, this phenomenon leads to the destruction of bridges, roads, power lines, and other engineering structures. Erosion processes in lowland river valleys are primarily characterized by the erosion of valley sides and the formation of ravines on valley slopes, often resulting in erosion craters beneath bridges at their supports and adjacent abutments. Furthermore, subsidence events in loess rock regions, specifically sandy loam, and dusty loam, occur in the foothill and foothill accumulative plains, where the extent of subsidence can reach up to 2 meters. These losses rock areas link to multiple focal points of ravine erosion and landslide formations. A fundamental

prerequisite for the initiation of landslides and mudslides is the presence of slopes, which essentially rely on relief energy. Even in cases of substantial rock moisture, landslides and mudslides will not occur in the absence of sloping terrain.

The region's topography exerts a significant influence on its local climate, which is shaped by the convergence of Arctic, Siberian, Iranian, and Central Asian air masses. The climate in the Almaty region, as a whole, exhibits continental characteristics, with distinct features attributed to both mountainous areas and plains. In the northern lowlands, the territory experiences significant diurnal and annual temperature fluctuations, characterized by cold winters and hot, arid summers. The mid-mountain zone enjoys a relatively temperate climate, while the highlands exhibit a more severe climate, with further climatic details available in Kairanbayeva, et al. [29].

According to the road-climatic zoning, the territory of the Almaty region belongs to the V road-climatic zone [30]. Table 1 presents the characteristics of the region.

Table 1.
The characteristics of the Almaty region's road-climatic zone.

Observed highest average daily amplitude of air temperature:	
• Cold month	-9.8
• Warm month	45
Average number of days per year with air temperature crossing 0°C	90
Daily solar radiation on the horizontal surface of the Earth in July, MJ/m²	886
Average relative humidity, %:	
• At 3 p.m. of the coldest month	75
• At 3 p.m. of the hottest month	38
High-speed standard headwind, m/s.	3.8
Prevailing wind directions, m/s:	
• December-February	S
• June-August	S
Maximum of average wind speeds in rhumbs per m/s:	
• January	1.3
• July	1.6
Standard depth of soil freezing, m:	
• Loam and clay	0.9
• Sandy loams, fine and dusty sands	1.1
• Gravelly, coarse and medium-sized sands	1.2
• Coarse-grained	1.4

The previous study presented the results of a survey conducted on a mountain road within the selected Almaty-Kosmostation region, covering a length of 26 kilometers. SAR interferometry was utilized for this purpose, enabling the assessment of extensive areas [31].

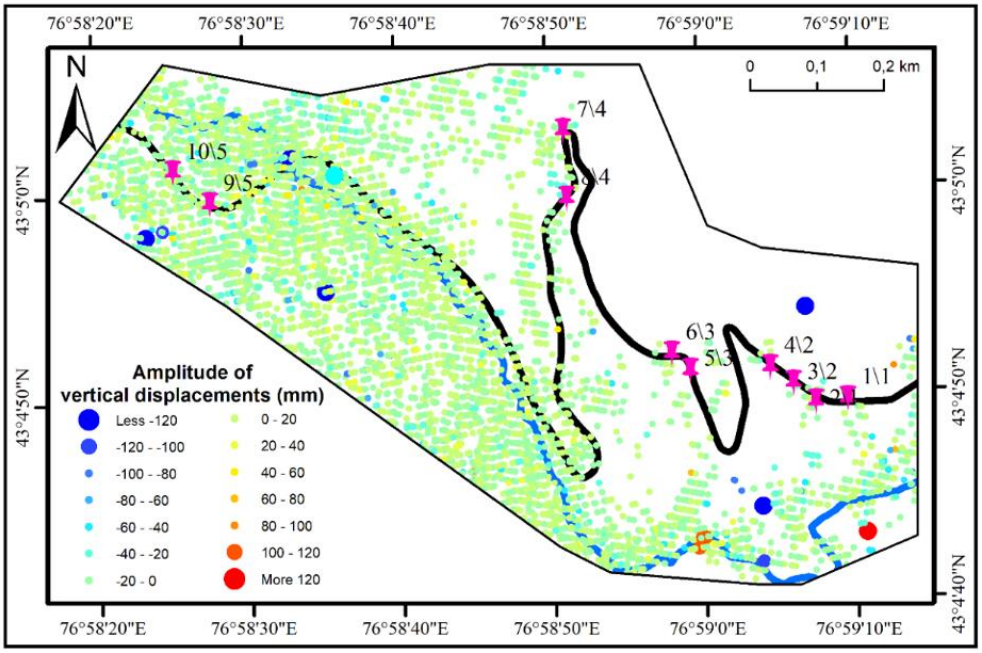

Figure 1.
Map of amplitude points of vertical displacements.

We employed a modified version of Persistent Scatterer Interferometry (PSI) to address the project's objectives, which involved processing 98 Sentinel-1 images for each orbit. These images spanned from April 2017 to May 2023. It was observed that approximately 90% of the surveyed points exhibited vertical displacements within the range of -20 to +20 millimeters (mm), indicating a relatively stable trend over the entire study period (Figure 1). Certain sections of the road, however, demonstrated gradual but consistent subsidence during the observation period, with amplitude of around 20mm over seven years. The most significant subsidence occurred in Section 4, reaching approximately 25 mm. The distribution of vertical displacement rates across the region indicated overall geodynamic stability, with values predominantly ranging from +5 to (-5) mm per year (Figure 2). We must acknowledge that various factors influence the road's condition, with precipitation being a key determinant. Therefore, the study of snow cover serves as an integral parameter for road monitoring.

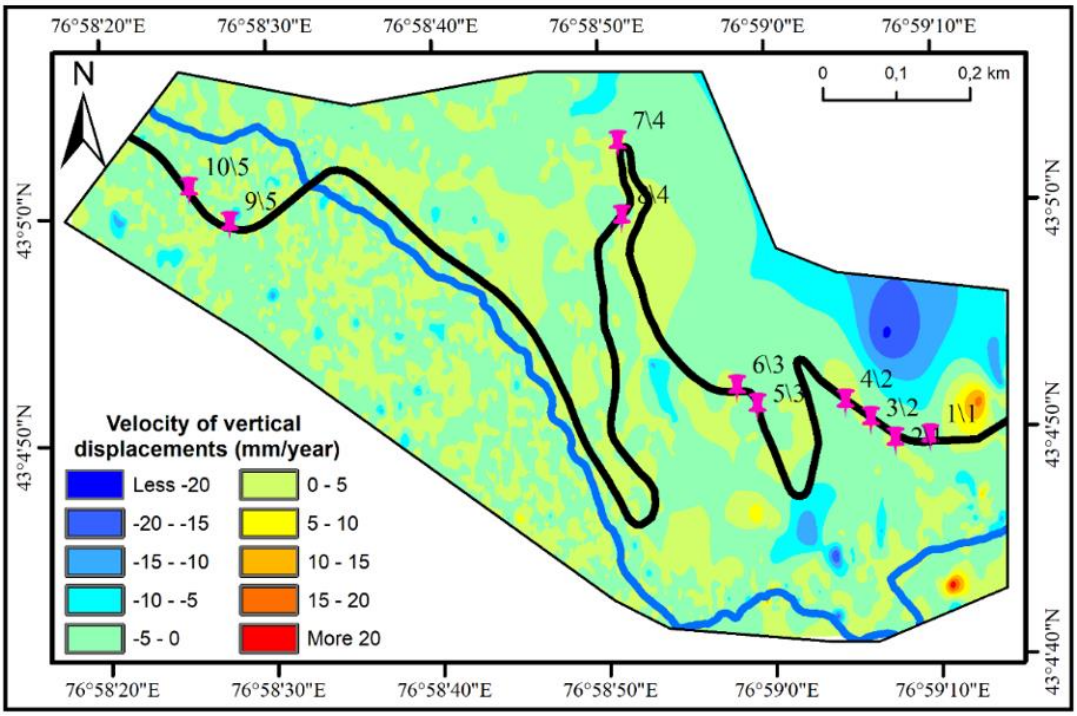

Figure 2.
Map of the distribution of vertical displacement velocity values.

The snow cover period in the study area typically spans from mid-November to early May. Recent years have observed a notable trend of rapid snowmelt in March, leading to damage to the road surface (Figure 3).

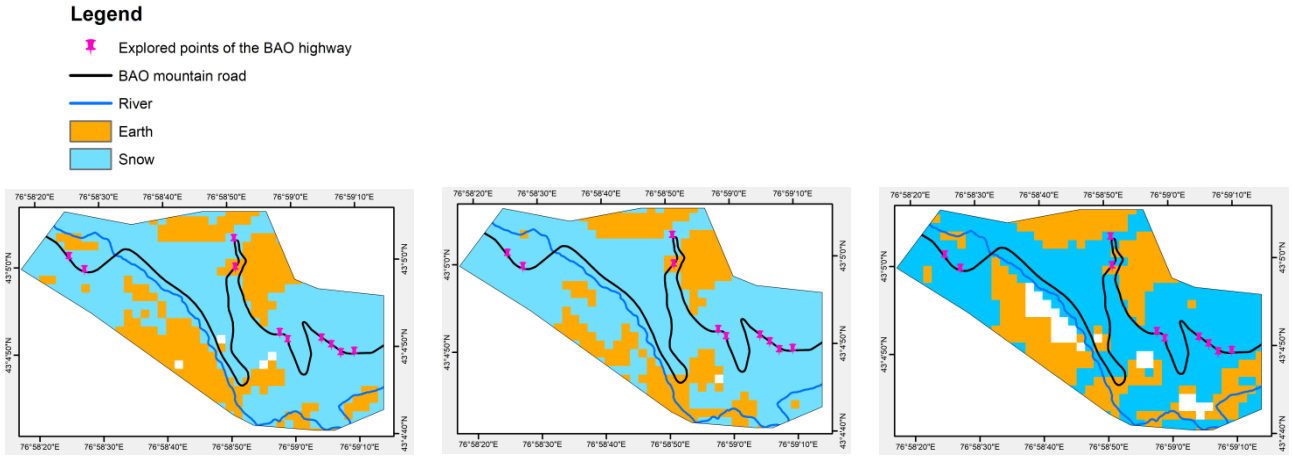

12.12.2022 13.12.2022 20.12.2022

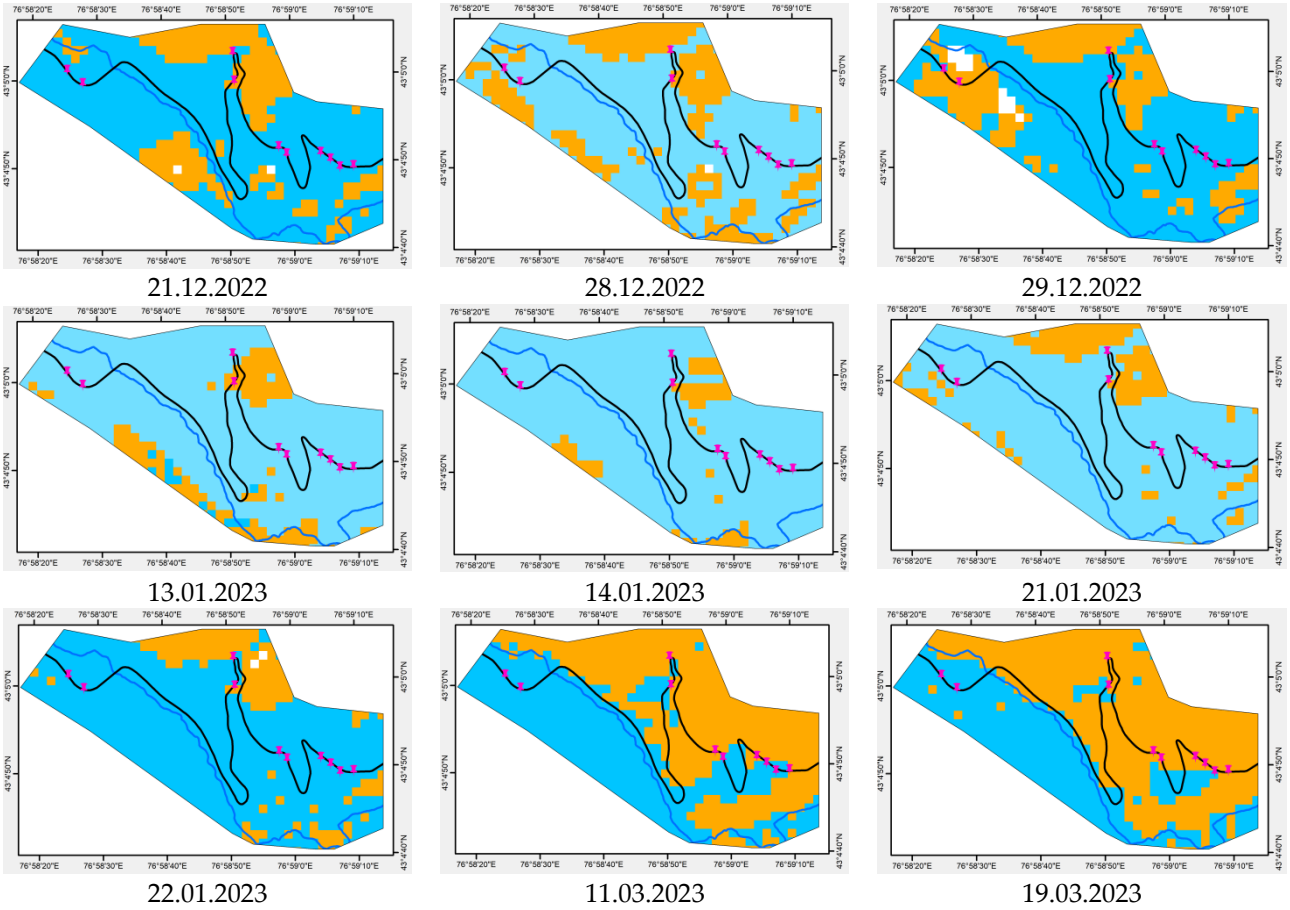

Figure 3.
Snow cover examples for the period of 2022-2023.

3. Methodology

As explained above, the current study is a part of the project aimed at developing an Intelligent Geographic Information System (IGIS) for predicting landslide occurrences and their effects on road technical and operational attributes. The article Kairanbayeva, et al. [29] details the general research methodology for this intelligent system. In Kazakhstan, as in other countries, the monitoring and assessment of road conditions strictly adhere to established state standards. As a result, all activities in the current research strictly adhere to these standards.

3.1. Methodology for Field Study of Road Conditions

In accordance with PR RK 218-27-2014 [32] road conditions are categorized into three classes. Category I corresponds to well-maintained roadways with a clear transverse profile, occasional single cracks may be present. Category II encompasses roads with 5-30% pavement deformation and alterations in road profile. Category II further subdivides into four subcategories: II/1 - smooth surface with no deformation, II/2 - minor deformations not affecting speed and safety, II/3 - small irregularities, occasional cracks, and other minor deformations, II/4 - significant irregularities, potholes, edge dips, and other deformations that significantly impact traffic and speed. Category III exhibits severe deformations in the form of a network of cracks and ruptures on the roadway.

Hence, as stipulated in reference ST RK 1219-2003 [33] meticulous road surface diagnostics are conducted during field surveys of brief road segments. The categorization of transverse cracks was performed based on their length intervals (e.g., 0-1 m, 1-2 m, etc.). Longitudinal cracks were grouped using a two-fold approach: initially, by their placement into axial, left, and right sides of the carriageway, and subsequently, by their overall length. Notably, the entire length of longitudinal cracks was documented.

Field measurements of the coefficients of adhesion were conducted using the IKSp-M device (Figure 4) in accordance with the specifications outlined in ST RK 1279-2013 [34].

Figure 4.
Portable device for measuring the friction coefficient namedIKSp-M and the measurement process.

Portable devices named IKSp-M are utilized for the selective measurement of the coefficient of adhesion values on road sections. Measurement requirements are:

- From 2 to 6 measurements per 1 kilometer of road;
- The left lane of each carriageway;
- On an artificially moistened surface;
- At an ambient temperature of about +20°C;
- Not during rain and not within 2-3 hours after precipitation.

Additional information about measuring devices and the methodology for studying the characteristics of the road surface can be found in Zh, et al. [35].

3.2. Laboratory Methods for Analyzing the Physical and Mechanical Properties of Asphalt Concrete

We extract specimens from pavement layers and use laboratory-prepared mixtures for analysis to assess the physical and mechanical properties of materials within pavement structures on road sections. This process necessitates the utilization of specific quality controls and auxiliary equipment, as outlined in ST RK 1218-2003 [36]. These include a drying oven, a bimetallic or electronic thermometer, a laboratory metal stirrer with temperature control, a core sampler or drilling rig, a shovel or scoop for sample collection, and receptacles. In the process of collecting samples from the structural layers of pavements, it is imperative to choose a segment of the surface located at a minimum distance of 0.5 m from the pavement's edge or road axis, with dimensions not exceeding 0.5 x 0.5 m. we extract these cylindrical cores using a drilling rig and then separate them into individual layers within the laboratory. We meticulously prepare standard samples from previously selected asphalt concrete samples to assess the strength of road surfaces. Subsequently, these cuttings or cores are subjected to controlled heating in a muffle furnace, reaching temperatures ranging from +165 to 180 ° C. In determining the density of the asphalt concrete pavement, it is necessary to measure the density of these cores. This process begins with the air-weighing of the samples. Subsequently, the asphalt concrete samples are immersed for a duration of 30 minutes in a container filled with water at least 20 mm above the surface of the samples at a temperature of approximately +20±2 ° C. Following this immersion, the samples are once again weighed, taking great care to prevent the formation of air bubbles on the samples. In the end, the samples are dried with a soft cloth and reweighed in air.

We calculate the sample's average density using the following formula:

$$P^{B} = g \cdot p/(g_2 - g_1), (1)$$

Where g represents the density of water, with g=1 g/cm^3; g_1 – s the mass of the sample suspended in water (g); g_2 – is the mass of the sample suspended in water for 30 minutes and then weighed in air (g). The grain composition of the mixture for pavement bases must adhere to the specified requirements outlined in Table 2 [37].

Table 2.
Specifications for mixtures used in the construction of pavement bases.

Mixture number	Maximum grain size D, mm	120	50	40	20	10	5	2,5	0,63	0,16	0,05
Coating mixtures											
C1	40	0	0	0-10	20-40	35-60	45-70	55-80	70-90	75-92	80-93
C2	20	0	0	0	0-10	10-35	25-50	35-65	55-80	65-90	75-92
Mixtures for bases (Continuous granulometry)											
C3	120	0-10	10-30	30-50	40-65	54-75	65-86	71-90	82-95	90-98	95-100
C4	80	0	0-10	15-35	28-55	40-70	50-80	60-85	80-65	91-97	95-100
C5	40	0	0	0-10	25-60	45-80	57-85	67-88	80-95	90-97	95-100
C6	20	0	0	0	0-10	25-60	50-77	58-85	80-95	90-97	95-100
C7	10	0	0	0	0-5	0-37	30-60	50-77	75-95	85-97	90-100
C8	5	0	0	0	0	0-5	0-40	20-55	88-87	75-98	90-100
Mixtures for bases (Intermittent granulometry)											
C9	80	0	0-10	15-35	28-55	40-70	50-80	50-80	60-88	85-97	95-100
C10	40	0	0	0-10	25-60	45-80	57-85	57-85	71-91	87-97	95-100
C11	20	0	0	0	0-10	25-60	50-77	50-77	70-88	85-97	95-100

Note: Mixtures C1 and C2 may be employed for base installation, provided an appropriate feasibility study has been conducted. Mixtures C3-C6 and C9-C11 are suitable for additional base layers, while C4-C5 and C10-C11 can be utilized for reinforcing road shoulders.
Mixtures C1 and C2, when used for surfacing, should comprise a minimum of 50% crushed stone from the total mass of particles exceeding 5 mm within the mixtures.

4. Results and Discussion

To assess the strength properties of pavements, studies were conducted on five sections, each measuring 50 meters in length, along the Almaty-Kosmostation highway, as illustrated in Figure 5, which contains the coordinates for the beginnings and ends of each section and their yellow marks [29].

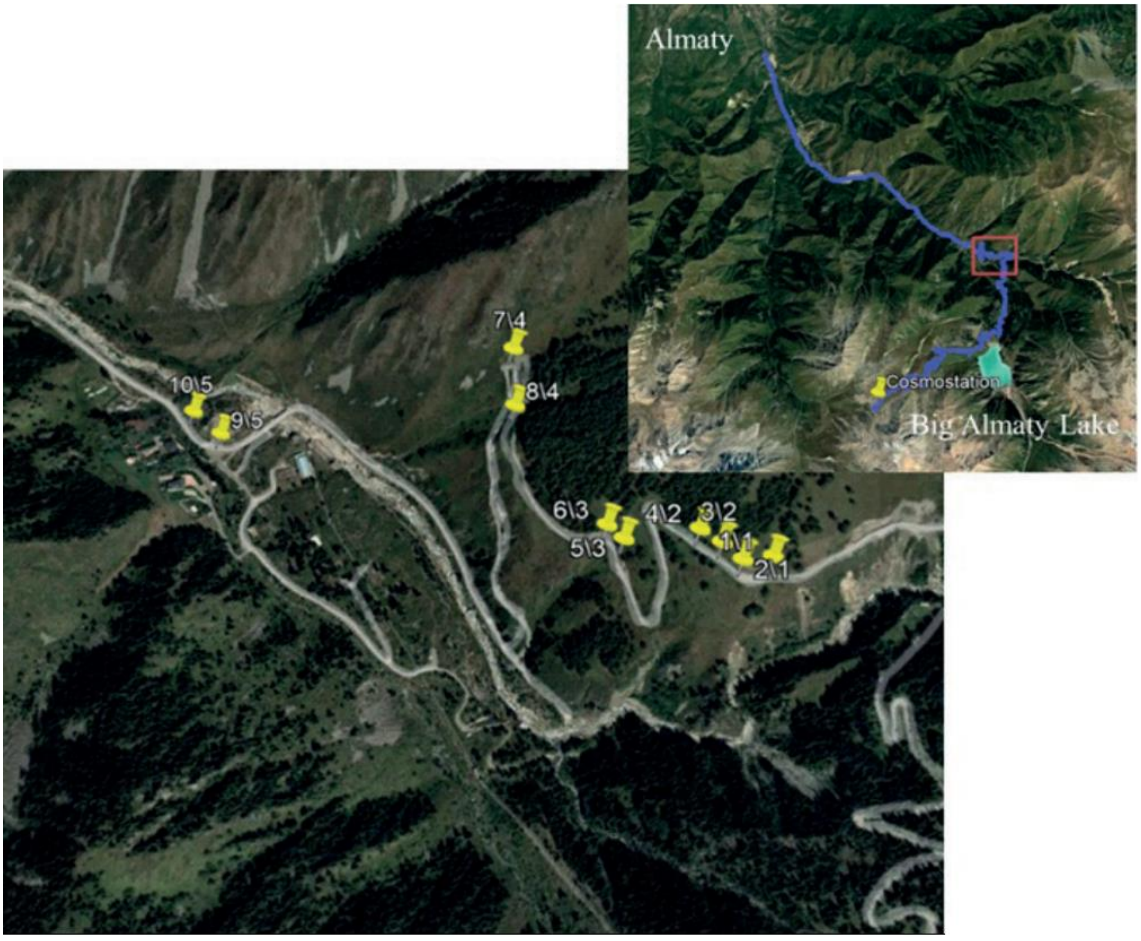

Figure 5.
The testing sections on the Almaty-Kosmostation road.

The first and the third sections exhibit a gentle slope. The second section is slightly steeper. The fourth section presents varying slopes on its sides. The fifth section traverses nearly level terrain and serves as a reference point.

Field studies such as visual assessments, adhesion coefficient measurements, core selection, etc. were conducted under clear weather conditions, with air temperatures fluctuating between +14°C and +20°C on May 19, 2021, and May 10, 2023.

Laboratory analysis of the physical and mechanical properties of asphalt concrete, conducted using selected cores, was performed at the Accredited Testing Laboratory of the Kazakh Automobile and Road Institute, known as L.B. Goncharov Institute.

The visual examination of the landslide body reveals its composition, consisting of coarse-clastic blocky-gravelly sand formations from the Upper Quaternary and modern ages (QIII-IV), originating from deluvial-proluvial processes. The significant presence of loose rocks can be attributed to the south-facing slope, which receives direct sunlight at a steep angle of 70-90°, causing rapid snowmelt, thereby minimizing snow cover even in snowy years.

The indigenous bedrock in the upper section of the slope undergoes substantial frost-induced weathering during the daily temperature fluctuations of the autumn-winter-spring seasons. The regelation processes, which involve nightly freezing and daytime thawing, contribute significantly to the rock's degradation compared to slopes with different orientations. Additionally, the annual precipitation, amounting to 300-400 mm per year, is predominantly absorbed into the landslide body. Over several years, this continuous moisture influx has increased the cumulative weight of sediments, leading to the formation of a water layer at the landslide's base. This water layer acts as a lubricant, facilitating the sliding of soil masses [38].

Several factors contribute to the swelling of roadways. Firstly, the landslide body, resting on the bedrock crossbar close to the landslide's "tongue," exerts pressure that contributes to the upward displacement of the roadbed. Secondly, the presence of water in the vicinity of the roadbed, which undergoes freezing and thawing cycles, also plays a role in this phenomenon. Furthermore, in the upper northeast region of the landslide body, secondary cracks have initiated (Figure 6). Notably, the primary slide crack, formed several years ago (5-10 years) (Figure 7), continues to expand gradually.

Figure 6.
Second-order tensile crack.

Figure 7.
Sliding cracks.

Table 3.
Granulometric composition of landslide sediments.

Location	Boulders 100-1000 mm and more, %	Macadam 10-100 mm, %	Rotted rock 1-10 mm, %	Sand 0,1-10 mm, %	Aleurite, sawing <-0,1mm, %
The upper ledge of the landslide	15	30	25	18	12
The middle part of the landslide	12	32	30	16	10
The lower part ("Tongue") of the landslide	10	35	35	8	12

Earlier studies aimed at investigate the geological structure of the region traversed by the Almaty-Kosmostation highway have revealed that the slope under examination is characterized by the predominant presence of various metamorphic, sedimentary, and magmatic formations from the Pre-Paleozoic and Paleozoic eras (Table 4). Mesozoic rocks are notably prevalent in intermontane depressions. Cenozoic deposits, on the other hand, are primarily found in inland and intermountain depressions, erosion valleys, and on mountain slopes. These deposits are typified by crystalline schists, quartzites, and, less frequently, gneisses with interlayers of marbles and amphiboles. Mountain ranges and intermontane depressions have been shaped by different tectonic movements. These movements have built up large layers of loosely lithified clastic formations.

Table 4.
Physical and mechanical properties of rocks of the metamorphic group of pre-Paleozoic and Paleozoic formations.

Indicators	Porphyrites. quartz porphyrites and dioriteporphyries	Effusives and pyroclasts. carbonate-siliceous schists	Carbonaceous-carbonate. carbonaceous-clayey shales
Particle density	2.90-3.01	2.73-2.75	2.71-3.11
	2.96 (31)	2.74 (14)	2.89 (9)
Density, t/m^3	2.65-2.91	2.66-2.81	2.04-3.40
	2.82 (31)	2.72 (14)	2.76 (9)
Porosity, %	2.4-8.6	0.7-0.75	0.7-13.8
	5.5 (31)	0.7 (14)	3.7 (9)
Tensile strength, 10^{-1} MPA:	2010-2899	1180-2610	526-3230
Compression	2640 (31)	1890 (17)	1860 (6)
Tensile	120-183	150-291	181-266
	169 (27)	221 (11)	232 (6)
Internal friction angle, degree	30-49	39-50	30-37
	37 (24)	45 (17)	32 (6)
Friction force, MPa	28.5-51.0	16.0-38.2	5.5-34.0
	38.2 (24)	27.2 (17)	0.6 (6)
Modulus of elasticity, MPa	0.5-0.9	0.5-0.9	0.5-1.2
	0.6 (38)	0.8 (17)	0.6 (6)
Poisson's ratio	0.19-0.25	0.18-0.30	0.24-0.35
	0.22 (38)	0.24 (17)	0.28 (6)

Based on the survey, the rate of evolutionary displacement does not surpass 0.6-1.1 meters per year, although it exhibits a persistent upward trend. Table 3 details the granulometric composition of the landslide soils, classifying them into the third category of mechanical development complexity.

The rocks on the slopes of the Ili Alatau mountains, where the investigated section of the Almaty-Space Station road is situated, exhibit the following properties: Medium and fine-grained granites have a dry rock compressive tensile strength ranging from 150 to 174 MPa; in a water-saturated state, this strength measures between 146 and 171 MPa; after undergoing 10 freezing cycles, it falls within the range of 139 to 169 MPa. These granites also display a softening coefficient of 0.94, a frost resistance of 0.07 to 0.16, and a water absorption rate of 0.18 to 0.32%. These parameters collectively classify the rocks belonging to all Paleozoic formations as exceptionally robust [39].

4.1. Results of Field Study of the Road Conditions

Table 5 presents the results of visual assessment and reveals a change in the visual assessment criteria from I/1 to I/4, indicating a deterioration in the condition of the road.

Table 5.
Results of the visual assessment of the pavement strength.

Section address, km+ to km+		Width of the road, m	Evaluation according to PR RK 218-27-2016		Description of deformations and destruction of pavement		Note
			2021 y.	2023y.	2021 y.	2023 y.	
0	1	9.5	I /1	I /2	There are no pronounced deformations		The appearance of small cracks increased from 20 to 60%
1	2	9.5	I /1	I /3			
2	3	9.5	I /1	I /3			
3	4	9.5	I /1	I /2-3			
4	5	8.0	I /1	I /4			
5	6	8.0	I/1	I/4			
6	7	8.0	I/1	I/2			
7	8	8,0	I/1	I/4			
8	9	7.5	I/3	I/4	Transverse cracks and irregularities		The number and size of longitudinal cracks increased by 20-30%
9	10	7.5	I/2-3	I/4			
10	11	7.5	I/2-3	I/3-4			
11	12	7.5	I/3-4	I/4			
12	13	7.5	I/4	I/4			
13	14				No visual assessment has been carried out on this site, construction work was underway		
14	15						
15	16						
16	17	7.2	I/1-2	I/4	A newly built section of the road. Transverse cracks are observed in increments of 2-3 m	The appearance of small transverse and longitudinal cracks increased by 2-3 times more	The increase in the number of cracks mainly depends on landslides of soil masses from mountain slopes

The escalation in the prevalence of cracking on various sections of the highway is not solely attributed to the region's climatic characteristics. The substantial impact of landslide materials from the mountain slopes significantly accelerates the cracking process on the road surface. Furthermore, the inadequate maintenance of the aforementioned road sections exacerbate the situation.

Table 6 presents the outcomes of crack assessments conducted in 2021 and 2023 for specific regions. Figures 8 and 9 depict histograms illustrating the progression in the quantity of transverse and longitudinal cracks over the course of three years of the highway's operation.

Table 6.
Results of field measurements to determine defects in the road surface.

Plot №	Number of popeper cracks, length					Total length of longitudinal cracks, m						Crack grid, pcs.		Note	
	0-1 m	1-2 m	2-3 m	3-4 m	4-5 m	r/b left side		r/b center		r/b right side					
	2021 y./2023 y.					2021 y.	2023 y.	2021 y.	2023 y.	2021 y.	2023 y.	2021 y.	2023 y.	2021 y.	2023 y.
1	6/14	3/12	1/9	0/6	0/11	∑11.5	∑21.2	∑16.9	∑25.1	∑12.1	∑16.6	2	2	-	Pitting amount increased
2	8/14	3/9	2/10	0/7	0/7	∑8	∑27.0	∑17.04	∑28.3	∑13.9	∑19.4	5	9	-	
3	7/21	6/16	3/17	2/8	0/6	∑17.8	∑24.6	∑19.25	∑31.6	∑7.4	∑14.8	3	8	Roadbed slope erosion	Same. Dangerous for vehicles
4	11/18	6/18	3/13	3/14	1/5	∑34.8	∑44.8	∑3.3	∑11.8	∑22.2	∑29.7	2	6		Same. Highly dangerous for vehicles
5	5/11	4/17	2/15	1/10	1/4	∑6.8	∑14.7	∑18.1	∑27.3	∑15.6	∑20.7	2 On the left side	5 On the same	-	-

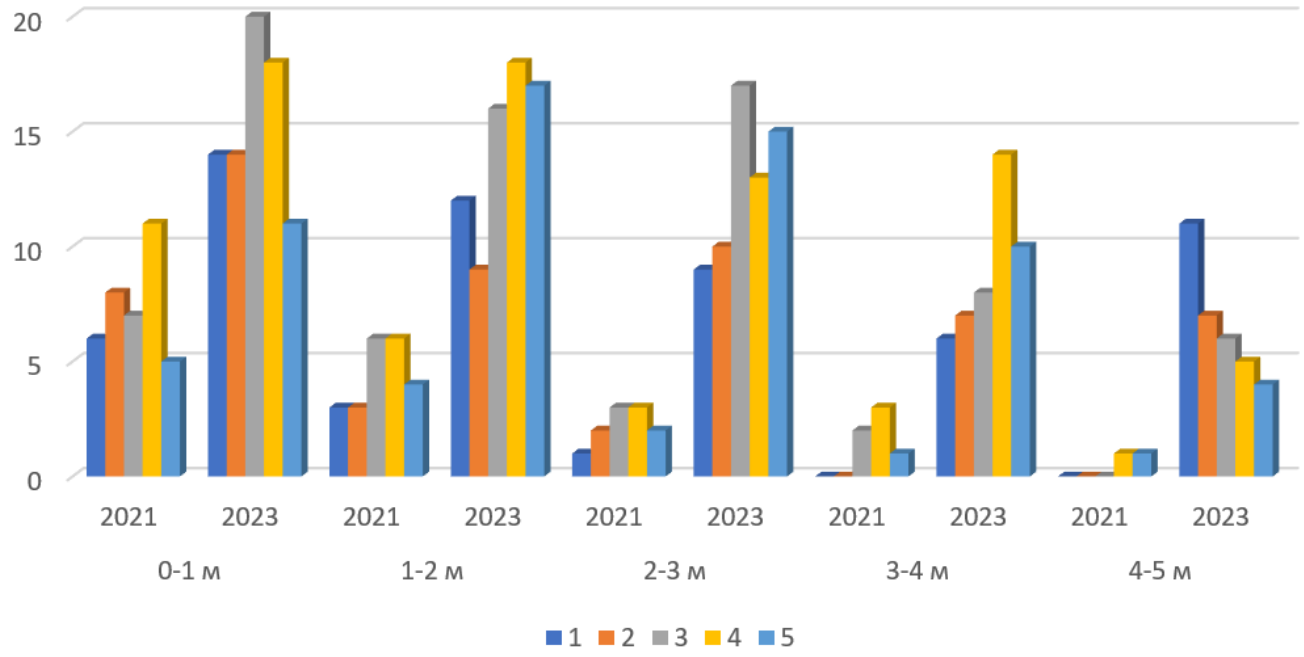

Figure 8.
The evolution in the quantity of transverse cracks over three years of the highway's operation.

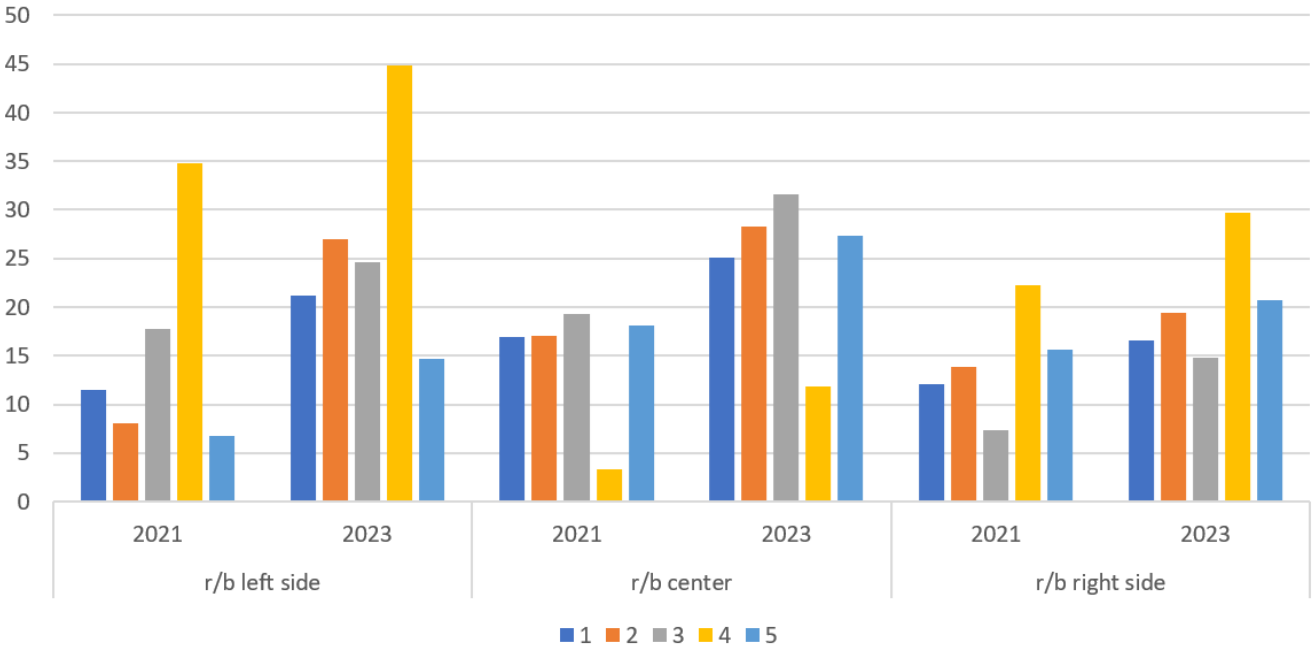

Figure 9.
The evolution in the length of longitudinal cracks along the sides of the roadbed.

A comparative analysis reveals a substantial increase in the total length of longitudinal cracks in 2023 compared to the results from 2021. Notably, areas No. 2 and 4 exhibit the most significant increase in the number of cracks.

Figure 10 illustrates the road damage that is characteristic of all segments of this road, signaling the onset of roadway deterioration. The sharp increase in the number of transverse cracks and the emergence of deep transverse and longitudinal cracks in site No. 2 can be attributed to the presence of sandy soils on the mountain slopes along this section (Figure 11). At site No. 3, the formation of transverse cracks exhibits a distinct pattern, particularly in terms of their length. Furthermore, this region has experienced noticeable slope erosion (Figure 12), with erosion levels increasing annually. Site No. 4 displays a different configuration in the development of longitudinal cracks (Figure 13). These longitudinal cracks do not align with the road axis or the travel lanes of the roadway; instead, they resemble deep, prominent lines. Numerous smaller crack lines coalesce to form a complex network of longitudinal cracks, positioned along the edge of the pavement. Despite the relatively short service life of newly constructed site No.5, which has been in operation since 2021, various types of cracks have already appeared on the surface of the pavement (Figure 14).

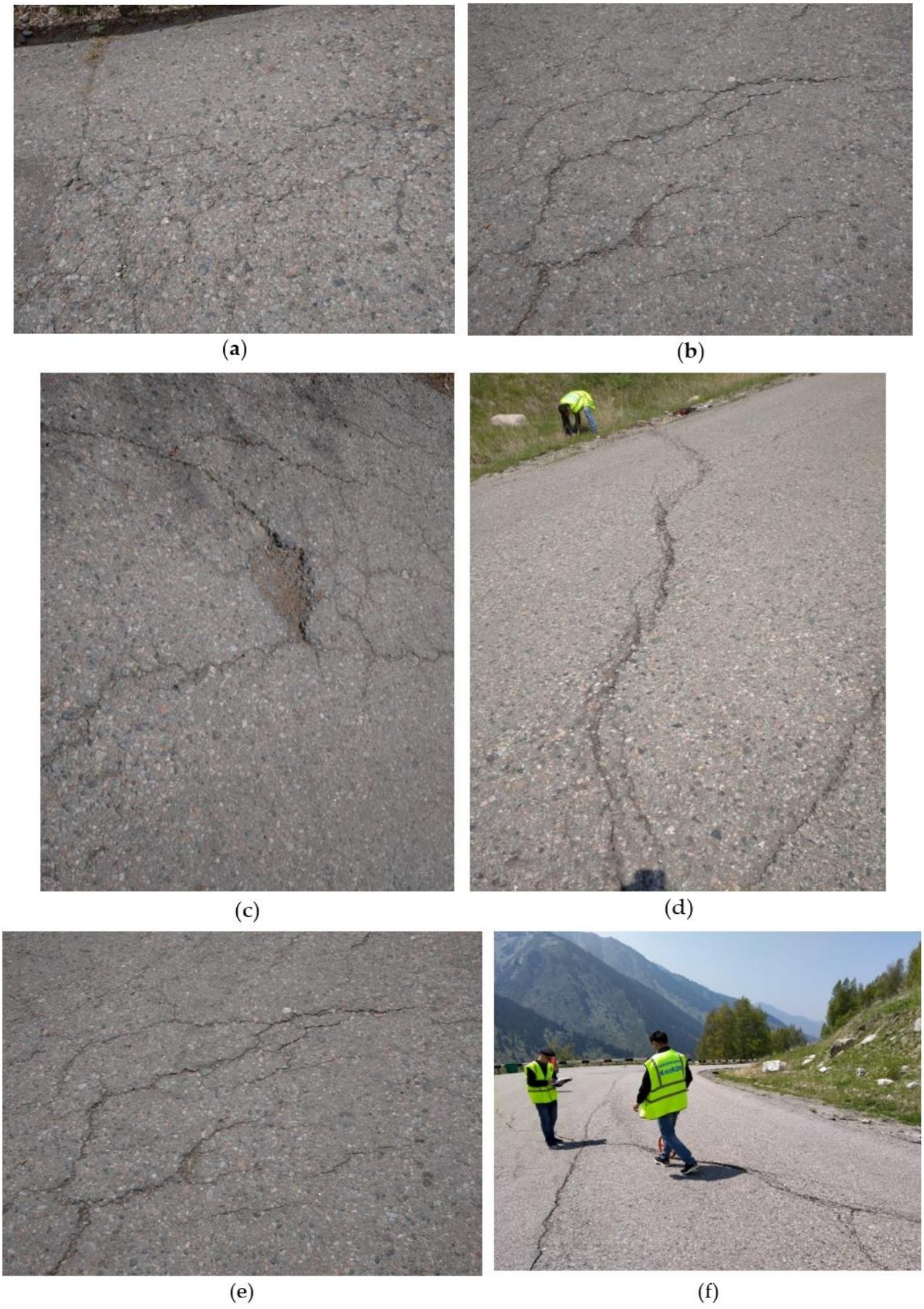

Figure 10.
Small (Starting) (a) and medium (b) crack grids, the formation of small holes in the middle of the crack grid (c), deep (Reflected) transverse cracks (d), multi-branch transverse cracks (e) and longitudinal cracks (f).

Figure 11.
Weak soils of mountain slopes, creating a shear force on the base of the pavement.

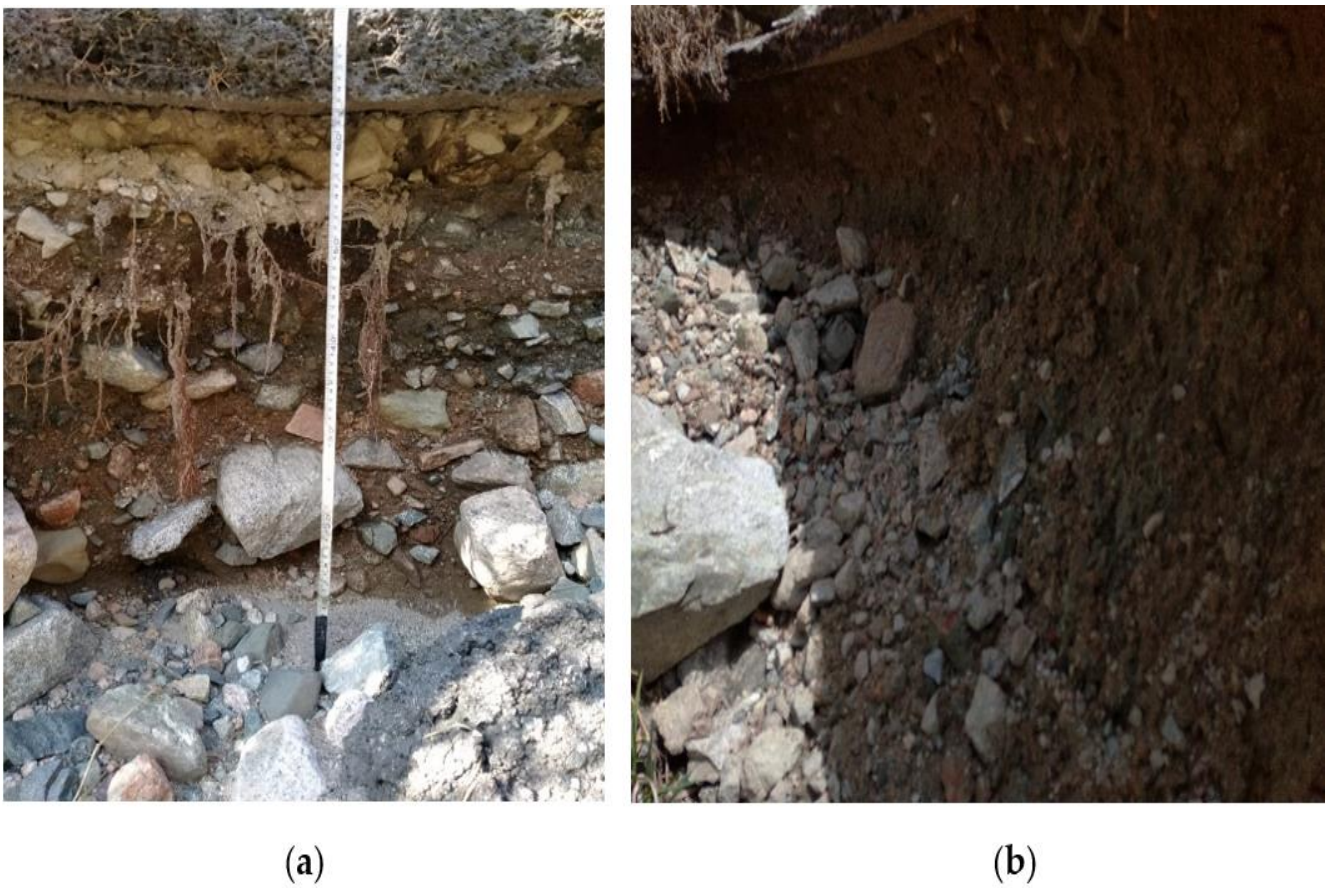

Figure 12.
General type of erosion in 2021 (a) and in 2023 (b).

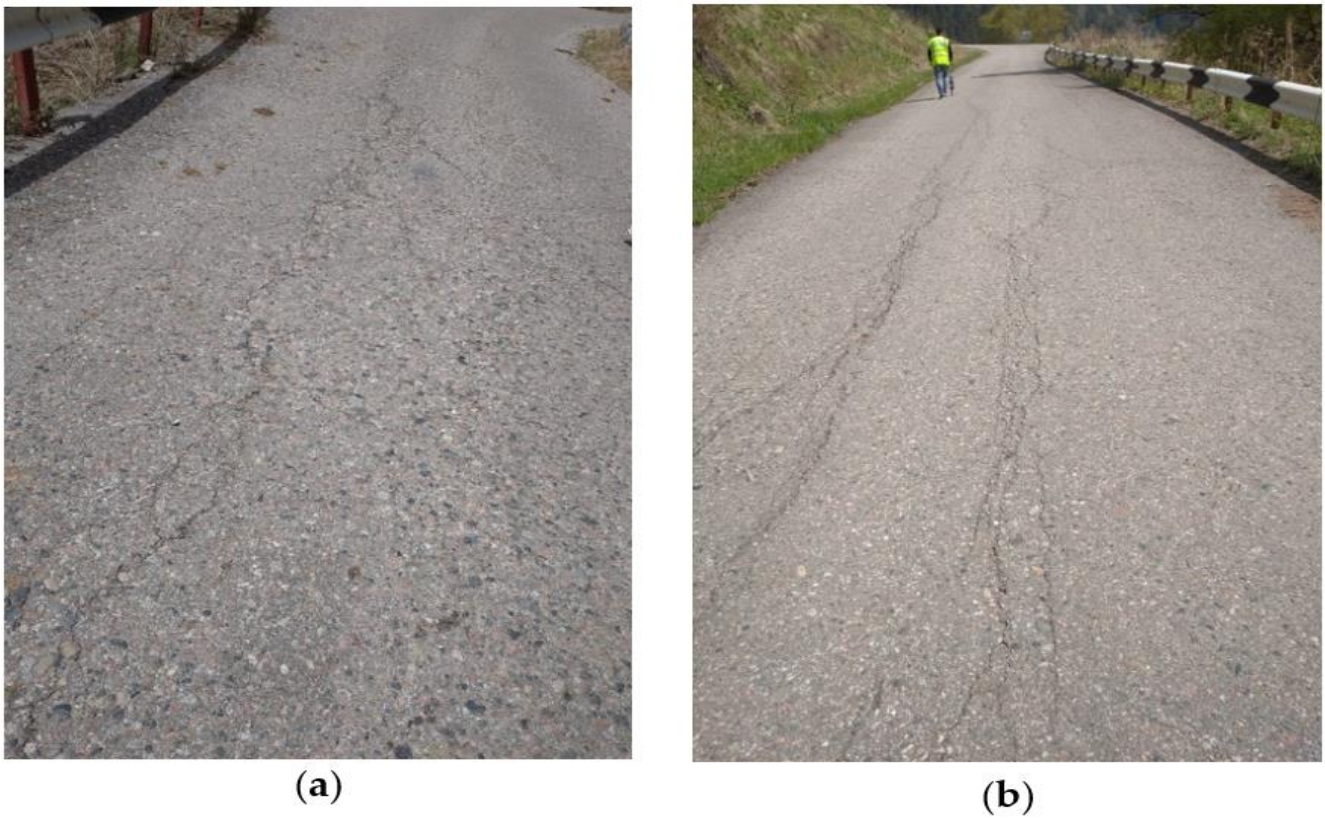

Figure 13.
Longitudinal cracks in section No. 4.

Figure 14.
Small cracks and pits that appeared on the surface of the newly built site No. 5.

Field measurements of adhesion coefficients were conducted in compliance with the stipulations outlined in ST RK 1279-2013. The results are presented in Table 7.

Table 7.
Results of measurements of coefficients of adhesion.

Plot no.	Measurement locations	Longitudinal clutches		Transverse clutches
		Forward direction	Reverse direction	
1	0-10 m	0.64	0.75	0.65
		0.56	0.76	0.66
		0.66	0.59	0.59
		0.71	0.64	0.74
		0.65	0.62	0.72
	Average	0.64	0.67	0.67
	10-20 M	0.65	0.72	0.7
		0.7	0.66	0.7
		0.67	0.75	0.67
		0.66	0.65	0.64
		0.65	0.63	0.65
	Average	0.67	0.68	0.67
	20-30 M	0.64	0.65	0.65
		0.76	0.75	0.71
		0.56	0.73	0.7
		0.72	0.76	0.71
		0.63	0.75	0.65
	Average	0.66	0.73	0.68
	30-40 M	0.66	0.75	0.65
		0.62	0.75	0.65
		0.75	0.64	0.74
		0.74	0.71	0.71
		0.64	0.77	0.73
	Average	0.68	0.72	0.7
	40-50 M	0.66	0.65	0.67
		0.66	0.81	0.71
		0.74	0.66	0.66
		0.75	0.66	0.66
		0.73	0.73	0.71
	Average	0.71	0.7	0.68
2	0-10 m	0.68	0.74	0.64
		0.66	0.67	0.67
		0.7	0.65	0.68
		0.75	0.72	0.72
		0.76	0.74	0.74
	Average	0.71	0.7	0.69
	10-20 M	0.69	0.77	0.67
		0.74	0.68	0.68
		0.74	0.71	0.71
		0.64	0.71	0.71
		0.73	0.75	0.7
	Average	0.71	0.72	0.69
	20-30 M	0.72	0.64	0.7
		0.72	0.65	0.65
		0.8	0.72	0.72
		0.58	0.66	0.66
		0.67	0.75	0.7
	Average	0.7	0.68	0.68
	30-40 M	0.73	0.65	0.65
		0.69	0.7	0.74
		0.71	0.63	0.63
		0.67	0.68	0.67
		0.65	0.66	0.66
	Average	0.69	0.66	0.67
	40-50 M	0.65	0.58	0.68
		0.77	0.73	0.72
		0.71	0.73	0.71
		0.72	0.74	0.64
		0.65	0.67	0.67
	Average	0.7	0.69	0.68
3	0-10 M	0.71	0.65	0.65
		0.72	0.75	0.65
		0.56	0.75	0.75

Plot no.	Measurement locations	Longitudinal clutches		Transverse clutches
		Forward direction	Reverse direction	
		0.66	0.68	0.68
		0.74	0.61	0.71
	Average	0.68	0.69	0.69
	10-20 M	0.73	0.72	0.66
		0.68	0.68	0.68
		0.66	0.73	0.66
		0.74	0.59	0.71
		0.74	0.69	0.74
	Average	0.71	0.68	0.69
	20-30 M	0.75	0.66	0.7
		0.69	0.71	0.67
		0.63	0.72	0.64
		0.63	0.67	0.63
		0.72	0.75	0.72
	Average	0.68	0.7	0.67
	30-40 M	0.73	0.67	0.66
		0.68	0.68	0.68
		0.72	0.7	0.72
		0.75	0.71	0.7
		0.72	0.72	0.72
	Average	0.72	0.69	0.7
	40-50 M	0.72	0.68	0.65
		0.7	0.69	0.7
		0.66	0.75	0.66
		0.67	0.71	0.67
		0.65	0.63	0.68
	Average	0.68	0.69	0.67
4	0-10 M	0.73	0.7	0.68
		0.69	0.66	0.69
		0.75	0.72	0.72
		0.59	0.69	0.59
		0.77	0.72	0.7
	Average	0.71	0.7	0.68
	10-20 M	0.73	0.58	0.67
		0.59	0.76	0.69
		0.67	0.75	0.71
		0.72	0.75	0.66
		0.71	0.64	0.7
	Average	0.68	0.7	0.68
	20-30 M	0.71	0.68	0.64
		0.67	0.66	0.67
		0.65	0.71	0.74
		0.75	0.71	0.69
		0.73	0.77	0.73
	Average	0.7	0.71	0.69
	30-40 M	0.68	0.74	0.68
		0.65	0.69	0.65
		0.67	0.72	0.71
		0.7	0.71	0.74
		0.71	0.66	0.59
	Average	0.68	0.7	0.67
	40-50 M	0.72	0.69	0.69
		0.7	0.66	0.66
		0.65	0.75	0.75
		0.65	0.69	0.68
		0.7	0.68	0.7
	Average	0.68	0.69	0.71
5	0-10 M	0.67	0.66	0.66
		0.72	0.76	0.73
		0.69	0.67	0.71
		0.67	0.59	0.69
		0.7	0.68	0.67
	Average	0.69	0.67	0.69
	10-20 M	0.66	0.77	0.7

Plot no.	Measurement locations	Longitudinal clutches		Transverse clutches
		Forward direction	Reverse direction	
		0.74	0.64	0.62
		0.66	0.63	0.66
		0.72	0.59	0.69
		0.67	0.59	0.7
	Average	0.69	0.64	0.67
	20-30 M	0.58	0.67	0.68
		0.65	0.67	0.61
		0.73	0.74	0.7
		0.65	0.73	0.64
		0.76	0.58	0.72
	Average	0.67	0.68	0.67
	30-40 M	0.71	0.72	0.72
		0.67	0.73	0.73
		0.64	0.59	0.59
		0.73	0.68	0.68
		0.7	0.74	0.7
	Average	0.69	0.69	0.68
	40-50 M	0.74	0.57	0.6
		0.74	0.66	0.64
		0.65	0.66	0.66
		0.64	0.74	0.71
		0.66	0.73	0.71
	Average	0.69	0.67	0.66
Interval of deviation of the average values of the coefficients of adhesion		0.64-0.71	0.64-0.73	0.67-0.70
Variance. %		5.6	12.3	4.3

The analysis of the results revealed that the lane on the opposite side of the road, specifically the lane adjacent to the hill, and the most unstable road surfaces, with adhesion coefficients ranging from 0.64 to 0.73 and a deviation of 12.3%. The adhesion coefficients on the road surface in both forward and reverse directions, as well as on the transverse profile, exhibit unstable characteristics, implying that the top layer of the pavement is nearly in a state of disrepair.

4.2. The Results of Laboratory Analysis of the Physical and Mechanical Properties of Asphalt Concrete

The laboratory analysis of materials extracted from the roadbed and base composed of sand-gravel blend (SGB) was conducted in conformity with the specifications outlined in ST RK 1290-2004 [40]. These measurements were carried out under specific environmental conditions, with an air temperature of 23°C and a relative humidity of 67%. We recorded the roadbed material's moisture content at 7.1%, while the base of the SGB showed a moisture content of 4.7%. The grain composition of the roadbed corresponded to the C10 mixture, whereas the base of the SGB was classified as the C5 mixture [41].

Table 8.
Laboratory analysis results of the physical and mechanical properties of asphalt concrete.

Name of indicators, units of measurement	Meaning of indicators		
	Standards by ST RK 1225	Actual values	
		Sample 1	Sample 2
Average density of the sample, g/cm^3	No standard	2.34	2.36
Water saturation, % by volume	From 2 to 5	5.28	5.33
Strength R50, MPa	Not less than 1.1	3.46	3.22
Strength R0, MPa	No more than 13.0	7.70	7.90
Strength R20, MPa	Not less than 2.2	4.71	4.76
Coefficient. water resistance,%	Not less than 0.85	0.80	0.81
Coefficient. core No. 1,%	0.99	0.96	0.93
Bitumen content, %	From 4.5 to 6.0	4.95	5.33
Grain composition:			
20	90-100	94.2	92.9
15	70-90	76.0	76.8
10	62-85	53.5	59.5
5	40-50	38.9	44.5
2,5	28-38	29.3	32.7
1,25	20-28	23.7	26.2
0,63	14-20	17.2	18.6
0,315	10-16	11.9	12.6
0,16	6-12	7.6	8.1
0,071	4-10	3.1	3.1

We extracted cylindrical cores through drilling to assess the physical and mechanical properties of the road surface assess the physical and mechanical properties of the road surface (Figure 15 a, b). In the laboratory, two standard samples were prepared from the collected asphalt concrete samples (Figure 15 c). We conducted laboratory testing procedures in accordance with the guidelines provided in GOST [42]. The findings from the laboratory analysis of the physical and mechanical properties of asphalt concrete can be found in Table 8 and Figure 16.

Figure 15. Asphalt concrete samples: (a) sampling in the field; (b) samples from 4 sections of the road under study; (c) reference materials prepared in the laboratory.

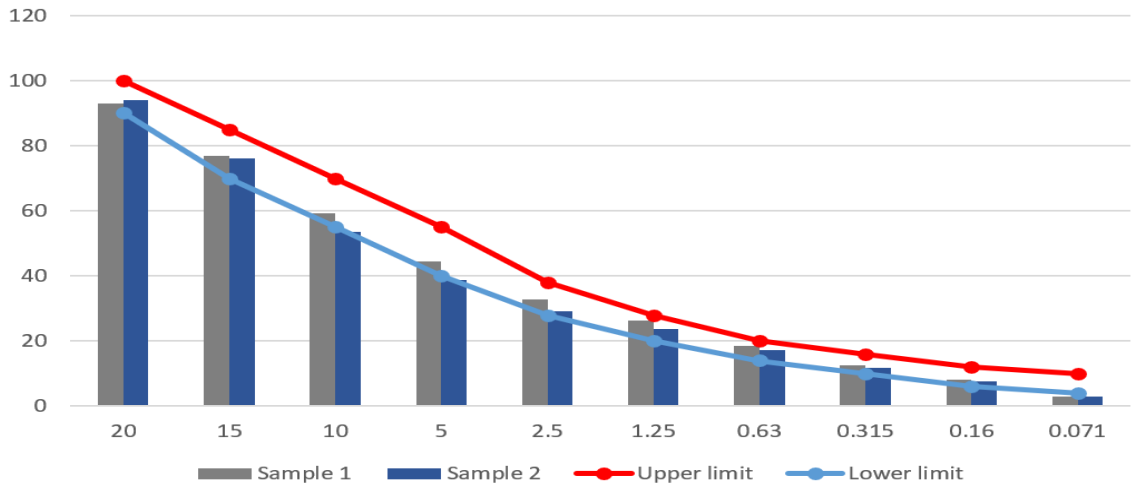

Figure 16.
Grain composition of fine-grained asphalt concrete.

The laboratory analysis results within the study areas reveal that the pavement's base is comprised of a single layer of natural sand-gravel blend (SGB) with a grade of C4-C6, which does not conform to the requirements specified in GOST [42]. The standards for base construction permit the use of mixtures C1 and C2, and employ mixtures C3-C6 and C9-C11 for additional base layers. Mixtures C4-C5 and C10-C11 are typically used for strengthening roadsides. It's worth noting that on the road under examination, the base materials and the natural mountain soil do not exhibit substantial differences.

The specified water saturation by volume should fall within the range of 2-5%. However, the actual water saturation of the investigated asphalt concrete mixture is higher, ranging from 5.28% to 5.33%. Furthermore, the water resistance coefficient should be at least 0.85%, but the test samples yielded values slightly below the requirement, at 0.80% and

0.81%. In the asphalt-concrete mixture, the volume of the fraction with a size of 0.071 mm should fall within the range of 4-10% of the total mass of the mixture. However, in the samples examined, the actual fraction does not exceed 3.11%.

4.3. Discussion of the Results of Field and Laboratory Studies

As pointed out in Abed, et al. [43] the Life Cycle Assessment (LCA) of asphalt pavements is subject to substantial uncertainty due to variations in the quantity and impact of individual components, data quality for each component, and the variability in the durability of asphalt concrete. As a result, the critical consideration of asphalt durability and uncertainty has the potential to profoundly influence LCA outcomes and interpretations.

Based on the findings of the adhesive property assessments of asphalt concrete mixtures presented in ST RK 1549-2006 [41] it has become evident that the adhesive strength of the material to bitumen is greatly influenced by the sources of the aggregates used in the asphalt concrete binder and the prevailing humidity conditions. It is notable that, even when the mineralogy and formation processes are similar, there can be substantial variations in the adhesive strength of bitumen. However, the incorporation of additives can mitigate the impact of moisture on bonding strength.

Moisture damage to asphalt pavements represents a complex phenomenon influenced by various factors, and it remains not entirely comprehended. People don't fully understand this because they don't know enough about three important topics: the main things that cause moisture damage in real life, the right way to do tests in the lab, and how well treatments work. Research conducted in AASHTOT [44] and Lu [45] has revealed that multiple factors, such as the air void content, road surface structure, total precipitation volume, asphalt mixture type, the utilization of additives, and the age of the road surface, exert a substantial influence on the extent of moisture damage. In these studies, laboratory experiments have demonstrated that a higher air void content not only allows for increased moisture ingress but also significantly diminishes fatigue strength under wet conditions.

As mentioned in the third section, the field and laboratory studies in this work were conducted in accordance with the state standards adopted in Kazakhstan.

We can draw the following conclusions based on the technical and operational characteristics of the road, as well as the laboratory studies of the chosen cores.

1. Cracking on the road sections is not solely a consequence of climatic factors but also correlates with the presence of landslide material from mountain slopes.
2. The unsatisfactory condition of the pavement and inadequate maintenance of road sections contribute to the exacerbation of the cracking process.
3. The lane on the opposite side, close to the hill, has the least stable road surfaces, with adhesive confidents ranging from 0.64 to 0.73.
4. The top layer of the pavement is deteriorating, which could lead to hazardous conditions on the road.
5. Transverse cracks and crack patterns form due to the low-strength properties of the materials used in the base layers.
6. The influence of shifting mountain masses and water flow from mountain slopes may be responsible for the appearance of "non-standard" transverse cracks.
7. Erosion of the roadbed slope has been ongoing since 2021, but the issue remains unaddressed, resulting in the complete closure of traffic in this section.
8. The laboratory analysis results reveal several significant findings: The base of the pavement in the studied areas is composed of a single layer of natural sand-gravel blend (SGB) with the grade of C4-C6, which falls short of meeting the prescribed requirements. The water saturation of the analyzed asphalt concrete mixture exceeds the recommended range of 5.28-5.33%, surpassing the ideal level of 2-5%. The water resistance coefficient also fails to meet the specified criteria, with actual values of 0.80% and 0.81%, in contrast to the required minimum of 0.85%. The fraction volume of 0.071 mm does not align with the prescribed range, as the studied samples indicate it does not surpass 3.11% of the total mixture weight. In summary, the laboratory analysis results collectively emphasize that the composition of materials on the studied road section does not adhere to the established requirements. Consequently, a complete replacement of these materials is necessary to ensure the requisite strength and stability of the road surface.

5. Conclusions

The Almaty-Kosmostation highway, which passes through the Ile-Alatau National Park, served as the research site. This park represents an exceptional natural complex situated in the Trans-Ili Alatau region, in the north-western part of the Tien Shan mountain range, and it is under state protection. The road experiences minimal traffic due to restrictions, resulting in a limited impact of vehicle activity on the road's condition. This unique circumstance allows for a more reliable examination of the influence of natural factors on the road's technical and operational state. A visual assessment has determined that, in accordance with the road classification adopted in Kazakhstan, this road falls into category 3 and exhibits significant deformations characterized by a network of cracks and breaks in the roadway. Additionally, the presence of "non-standard" transverse cracks is notable, and the influence of shifting mountain masses and the flow of water from the mountain slopes may link these unusual cracks. The coefficient of adhesion was determined using the device named IKSp-M on a surface that was moistened, with measurements conducted at the designated temperature of +20°C. The least stable road surfaces, characterized by a coefficient of adhesion ranging from 0.64 to 0.73, are predominantly observed in the opposite lane situated in close proximity to the hill. Mountain range shifts and water flow from the mountain slopes may influence this observation. Laboratory studies involved the collection of material samples from the roadbed's structural layers in the form of drilled cylindrical cores, which were then segregated into individual

layers upon reaching the laboratory. The determination of the physical and mechanical properties of the asphalt concrete was carried out at the Accredited Testing Laboratory of the Kazakh Automobile and Road Institute, named after L.B. Goncharov. The conclusion drawn from the laboratory analysis is that the materials used for the pavement do not comply with the stipulated requirements. The base comprises only one layer of natural sand-gravel blend (SGB), which is insufficient to ensure the necessary strength and stability of the road. Moreover, the water saturation of the studied asphalt concrete mixture exceeds the recommended level, which can lead to adverse consequences such as cracks and pavement deterioration. The water resistance coefficient also falls below the required value, contributing to the softening and deformation of the material in humid conditions. The fraction of 0.071 mm also fails to meet the established standards, potentially undermining the quality and durability of the road surface. In light of these findings, a comprehensive replacement of materials is imperative to guarantee the adequate strength and stability of the road surface.

The current study is a component of the broader project titled "Development of an Intelligent Geographic Information System (IGIS) for Forecasting Landslide Processes and Their Impact on the Technical and Operational Characteristics of Roads in Mountainous Areas." This initiative involves the utilization of meteorological data, processed satellite imagery, and field studies conducted during 2021-2022 to develop and train forecast models. These models serve as the foundation for IGIS. All collected and processed data will be integrated into this IGIS and utilized by two selected forecast models. These models, in turn, generate forecasts for the condition of specific road sections. The forecasts are presented in the form of ten parameters, which are recognized in the road sector of Kazakhstan for assessing road conditions. Consequently, through the newly established IGIS, upon entering the coordinates of a particular road section, users can access a forecast regarding the road surface condition. This forecast encompasses the number of transverse cracks falling within specific size ranges (0.1 m, 1-2 m, 2-3 m, 3-4 m, 4-5 m), the cumulative quantities of longitudinal cracks on the left side, right side, and along the road axis, as well as the count of crack grids.

The findings from both the field and laboratory investigations conducted in 2023 will serve as valuable input for refining and optimizing the forecast model of IGIS. We will also use these results to construct a risk map for the road section under examination. We will develop this map by extrapolating the predicted data into the future, which will enable a more comprehensive assessment of potential risks and road conditions.

References

[1] M. Santamaria-Ariza, H. S. Sousa, J. C. Matos, and M. H. Faber, "An exploratory bibliometric analysis of risk, resilience, and sustainability management of transport infrastructure systems," *International Journal of Disaster Risk Reduction,* vol. 97, pp. e104063-e104063, 2023. https://doi.org/10.1016/j.ijdrr.2023.104063

[2] V. Mymrin *et al.*, "Efficient road base material from Kazakhstan's natural loam strengthened by ground cooled ferrous slag activated by lime production waste," *Journal of Cleaner Production,* vol. 231, pp. 1428-1436, 2019. https://doi.org/10.1016/j.jclepro.2019.05.250

[3] Car Roads of Kazakhstan, "Car roads of Kazakhstan," Retrieved: https://www.gov.kz/memleket/entities/roads/activities/252?lang=ru. 2023.

[4] A. Pantuso, G. Loprencipe, G. Bonin, and B. B. Teltayev, "Analysis of pavement condition survey data for effective implementation of a network level pavement management program for Kazakhstan," *Sustainability,* vol. 11, no. 3, p. 901, 2019. https://doi.org/10.3390/su11030901

[5] H. Wang, W. Zhang, Y. Zhang, and J. Xu, "A bibliometric review on stability and reinforcement of special soil subgrade based on CiteSpace," *Journal of Traffic and Transportation Engineering (English Edition),* vol. 9, no. 2, pp. 223-243, 2022. https://doi.org/10.1016/j.jtte.2021.07.005

[6] Y. Li, Y. Chen, and Z. Li, "Climate and topographic controls on snow phenology dynamics in the Tienshan Mountains, Central Asia," *Atmospheric Research,* vol. 236, p. 104813, 2020. https://doi.org/10.1016/j.atmosres.2019.104813

[7] C. Luu *et al.*, "Flash flood and landslide susceptibility analysis for a mountainous roadway in Vietnam using spatial modeling," *Quaternary Science Advances,* vol. 11, p. 100083, 2023. https://doi.org/10.1016/j.qsa.2023.100083

[8] S. P. Pradhan and T. Siddique, "Stability assessment of landslide-prone road cut rock slopes in Himalayan terrain: A finite element method based approach," *Journal of Rock Mechanics and Geotechnical Engineering,* vol. 12, no. 1, pp. 59-73, 2020. https://doi.org/10.1016/j.jrmge.2018.12.018

[9] C. Wang *et al.*, "Unpaved road erosion after heavy storms in mountain areas of northern China," *International Soil and Water Conservation Research,* vol. 10, no. 1, pp. 29-37, 2022. https://doi.org/10.1016/j.iswcr.2021.04.012

[10] H. Soenen, S. Vansteenkiste, and P. Kara De Maeijer, "Fundamental approaches to predict moisture damage in asphalt mixtures: State-of-the-art review," *Infrastructures,* vol. 5, no. 2, p. 20, 2020. https://doi.org/10.3390/infrastructures5020020

[11] Technical, "Technical report of KazdorNII JSC on the results of determining the level of danger of landslide arrays on the section of the Zharkent–Koktal-Arasan highway Almaty, Republic of Kazakhstan." Almaty: KazdorNII, 2009, p. 203.

[12] W. F. Flora, "Development of a structural index for pavement management: An exploratory analysis," Master's Thesis. Purdue University, West Lafayette, Indiana, 2009.

[13] S. W. Katicha, S. Ercisli, G. W. Flintsch, J. M. Bryce, and B. K. Diefenderfer, "Development of enhanced pavement deterioration curves," Virginia Transportation Research Council (VTRC). (No. VTRC 17-R7), 2016.

[14] J. M. Bryce, G. W. Flintsch, S. W. Katicha, B. K. Diefenderfer, and A. Sarant, "Development of pavement structural capacity requirements for innovative pavement decision-making and contracting: Phase II," Virginia Transportation Research Council. (No. FHWA/VTRC 16-R20), 2016.

[15] S. Shrestha, S. W. Katicha, G. W. Flintsch, and S. Thyagarajan, "Application of traffic speed deflectometer for network-level pavement management," *Transportation Research Record*, vol. 2672, no. 40, pp. 348-359, 2018.

[16] M. L. Wang and R. Birken, *Sensing solutions for assessing and monitoring roads. In Sensor Technologies for Civil Infrastructures*. Woodhead Publishing. https://doi.org/10.1533/9781782422433.2.461, 2022, pp. 299-330.

[17] M. D. Todd, *Sensor data acquisition systems and architectures in sensor technologies for civil infrastructures*, Woodhead Publishing, pp. 19-49, 2022. https://doi.org/10.1016/B978-0-08-102696-0.00012-9

[18] National Academies of Sciences Engineering and Medicine, *Pavement management applications using geographic information systems*. Washington, DC: The National Academies Press. https://doi.org/10.17226/23344, 2004.
[19] G. Zhou, L. Wang, D. Wang, and S. Reichle, "Integration of GIS and data mining technology to enhance the pavement management decision making," *Journal of Transportation Engineering*, vol. 136, no. 4, pp. 332-341, 2010. https://doi.org/10.1061/(asce)te.1943-5436.0000092
[20] M. Maimaitiyiming *et al.*, "Effects of green space spatial pattern on land surface temperature: Implications for sustainable urban planning and climate change adaptation," *ISPRS Journal of Photogrammetry and Remote Sensing*, vol. 89, pp. 59-66, 2014. https://doi.org/10.1016/j.isprsjprs.2013.12.010
[21] M. M. Nielsen, "Remote sensing for urban planning and management: The use of window-independent context segmentation to extract urban features in Stockholm," *Computers, Environment and Urban Systems*, vol. 52, pp. 1-9, 2015.
[22] S. Behzadi and A. A. Alesheikh, "Introducing a novel model of belief–desire–intention agent for urban land use planning," *Engineering Applications of Artificial Intelligence*, vol. 26, no. 9, pp. 2028-2044, 2013. https://doi.org/10.1016/j.engappai.2013.06.015
[23] S. A. Beykaei, M. Zhong, and Y. Zhang, "Development of a land use extraction expert system through morphological and spatial arrangement analysis," *Engineering Applications of Artificial Intelligence*, vol. 37, pp. 221-235, 2015. https://doi.org/10.1016/j.engappai.2014.08.006
[24] S. A. Beykaei, M. Zhong, S. Shiravi, and Y. Zhang, "A hierarchical rule-based land use extraction system using geographic and remotely sensed data: A case study for residential uses," *Transportation Research Part C: Emerging Technologies*, vol. 47, pp. 155-167, 2014. https://doi.org/10.1016/j.trc.2014.06.012
[25] Weather Data, "Weather data," Retrieved: http://meteocenter.net. 2023.
[26] A. R. Medeu *et al.*, "Moraine-dammed glacial lakes and threat of glacial debris flows in South-East Kazakhstan," *Earth-Science Reviews*, vol. 229, p. 103999, 2022. https://doi.org/10.1016/j.earscirev.2022.103999
[27] T. Pánek, "Landslides and related sediments," *Encyclopedia of Geology*, vol. 2, pp. 708–728, 2021. https://doi.org/10.1016/b978-0-12-409548-9.12529-1
[28] A. Strom and K. Abdrakhmatov, "Rockslides and rock avalanches of Central Asia: Distribution, morphology, and internal structure," Elsevier. https://doi.org/10.1016/B978-0-12-803204-6.00002-8, 2018, pp. 7-12.
[29] A. Kairanbayeva *et al.*, "Impact of landscape factors on automobile road deformation patterns—a case study of the Almaty Mountain Road," *Sustainability*, vol. 14, no. 22, p. 15466, 2022.
[30] SP RK 2.04-01-2017, "State standards in the field of architecture, urban planning and construction, code of rules of the Republic of Kazakhstan. construction climatology. Astana, 2017," Retrieved: https://online.zakon.kz/Document/?doc_id=33546556. 2023.
[31] Z. Zhantayev, D. Talgarbayeva, A. Kairanbayeva, D. Panyukova, and K. Turekulova, "Complex processing of earth remote sensing data for prediction of landslide processes on roads in mountain area," *News of the National Academy of Sciences of the Republic of Kazakhstan, Series of Geology and Technical Sciences*, vol. 3, pp. 181–197, 2022.
[32] PR RK 218-27-2014, "Instructions for diagnosing and assessing the transport and operational condition of highways' with amendments and additions as of December 25, 2020," Retrieved: https://online.zakon.kz/Document/?doc_id=37657859. 2023.
[33] ST RK 1219-2003, "Roads and airfields. Methods for measuring unevenness of bases and coatings," Retrieved: https://online.zakon.kz/Document/?doc_id=30023388. 2023.
[34] ST RK 1279-2013, "Roads and airfields. Methods for determining the roughness of the road surface and the coefficient of adhesion between the wheels of a car and the road surface," Retrieved: https://online.zakon.kz/Document/?doc_id=32776999. 2023.
[35] Z. Zh, A. Kairanbayeva, A. Kiyalbayev, G. Nurpeissova, and D. Panyukova, "Data collection for intellectual forecasting: Metthods and results," *News of the NAS RK. Physics and Mathematics Series*, no. 4, pp. 108-117, 2021. https://doi.org/10.32014/2021.2518-1726.72
[36] ST RK 1218-2003, "Materials based on organic binders for road and airfield construction. Test methods," Retrieved: https://online.zakon.kz/Document/?doc_id=30023718. 2023.
[37] GOST 007-2009, "Mixtures of crushed stone-gravel-sand for coatings and bases of highways and airfields technical conditions," Retrieved: https://online.zakon.kz/Document/?doc_id=30829027. 2023.
[38] K. G. P. V. V. Bondarika, *YarSU named after A. Engineering geodynamics*. Moscow, Russian Federation: University Publishing House, 2007.
[39] V. S. Fedorenko, *Mountain landslides and landslides their forecasts*. Moscow, Russian Federation: MSU Publishing House, 1988.
[40] ST RK 1290-2004, "Soils. Methods for laboratory determination of physical characteristics," Retrieved: https://online.zakon.kz/Document/?doc_id=30092368. 2023.
[41] ST RK 1549-2006, "Mixtures of crushed stone-gravel-sand and crushed stone for coatings and foundations of highways and airfields. Technical specifications," Retrieved: https://online.zakon.kz/Document/?doc_id=30210186. 2023.
[42] GOST, "GOST 25607-2009 Crushed stone-gravel-sand mixtures for coatings and foundations of highways and airfields. Specifications - docs.cntd.ru," Retrieved: https://docs.cntd.ru/document/1200078691. 2023.
[43] A. Abed *et al.*, "Uncertainty analysis of life cycle assessment of asphalt surfacings," *Road Materials and Pavement Design*, vol. 25, no. 2, pp. 219-238, 2024. https://doi.org/10.1080/14680629.2023.2199882
[44] AASHTOT, "AASHTOT 283: Standard method of test for resistance of compacted asphalt mixtures to moisture-induced damage," Retrieved: https://global.ihs.com/doc_detail.cfm?document_name=AASHTO%20T%20283&item_s_key=00489198. 2023.
[45] Q. Lu, "Investigation of conditions for moisture damage in asphalt concrete and appropriate laboratory test methods," Doctoral Dissertation, University of California, Berkeley, 2005.